Platinum Testbeds: Interaction with Oxygen

Lina R. Saenz,[†] Perla B. Balbuena,*[,†] and Jorge M. Seminario*[,†,‡]

Department of Chemical Engineering, and Department of Electrical and Computer Engineering, Texas A&M University, College Station, Texas

Received: July 24, 2006; In Final Form: August 24, 2006

We develop testbeds to study catalytic reactions modeled using the minimum number of platinum atoms needed to have an acceptable description of the chemistry on a realistic platinum surface that may include the contribution from a bulk continuum or may simply represent a local site on a nanocluster. In this particular case, the requirement is that a stable cluster may be connected to a stable bulk with equivalent highest occupied molecular orbital and Fermi level, respectively. We focus our work on the interaction of platinum clusters with molecular oxygen, which yields a complex cluster−molecule with fully delocalized molecular orbitals in the neighborhood of the Fermi energy of platinum, responsible for the interesting catalytic behavior of this material.

I. Introduction

Detailed studies of platinum clusters and their interactions with reactant molecules are important for numerous applications such as fuel-cell catalysis and electrocatalysis.[1] Platinum is widely used in the catalysis industry due to its smaller hydrogenation energy compared with that of Ni and Pd.[2,3] Transition-metal clusters are used as models for catalytic surfaces, providing insights into the influence of the size and the structure[4] on reactivity.[5] Specific interactions of small molecules such as H_2, CO, and O_2 with such clusters have been reported.[2,6]

Small platinum clusters have been extensively investigated; however, the studies have been restricted due to the complexity of the Pt electronic structure.[7] Recent work reported density-functional-theory (DFT) analyses of bare and hydrogenated platinum clusters,[1] using Gaussian atomic-orbital methods within the generalized gradient approximation for the exchange and correlation. Sebetci and Güvenç[6] studied the lowest-energy structures of Pt_n clusters with molecular dynamics (MD) and thermal quenching (TQ) simulations by using a semiempirical version of an embedded-atom model (EAM). The non-self-consistent Harris functional version of the local density approximation (LDA) was used to study smaller clusters and Pt_{13},[8] which have drawn much attention because the existence of closed-shell icosahedral and cubooctahedral structures was reported.[4] Grönbeck and Andreoni reported a study of Au_2−Au_5 and Pt_2−Pt_5 clusters with DFT for the neutral and anionic states, using both the local-spin-density approximation (LSDA) for the exchange-correlation functional and the spin-polarized gradient-corrected Becke−Lee−Yang−Parr (BLYP) functional.[7]

Balasubramanian presented complete-active-space MCSCF followed by MRSDCI calculations to seek the electronic states of PtH_2.[3] Later, CASSSCF/first-order CI and second-order CI calculations for PtH were carried out by Balasubramanian and Feng.[9] Pt trimer was studied by Wang and Carter[10] using generalized-valence-bond with configuration-interaction (GVB/CI) calculations. A comparison between Au and Pt heptamers using DFT calculations employing relativistic core pseudopotentials with Gaussian basis and plane-wave pseudopotential was reported in ref 11. Also, Andrew and Wang[5] performed DFT calculations to study platinum hydrides and used a laser-ablation technique to get the infrared spectra of PtH_2, PtHD, and PtD_2. An early study carried out by Wang and Pitzer[12] using relativistic-electronic-structure calculations for the ground and excited states of PtH and PtH^+ found significant differences with experimental data. Okamoto[13] reported a study of adsorption of CO, O_2, H, and O on icosahedral clusters, which have corresponding (111) flat surfaces. A periodic DFT-GGA study of CO and OH adsorption on a variety of Pt−Ru alloy surfaces is carried out in ref 14.

In this work our goal is to find out about a few Pt clusters with characteristics compatible with the corresponding bulk material such that they can be combined with bulk ab initio models to study the chemistry taking place in a local site of a material. We test these clusters by interacting them with an oxygen molecule. The next section describes the methodology used for our analysis, and the results are described in section III.

II. Methodology

Structural optimization is carried out using the Berny algorithm[15] which calculates the derivatives of the energy with respect to the Cartesian coordinates of all atoms, ensuring that the atomistic system is in equilibrium, that is, forces are approximately zero in all atoms. These optimizations are followed by a second-derivative calculation performed to determine the existence of a true local minimum and to find zero-point energies. If negative eigenvalues are found in the Hessian matrix, the geometry is modified in order to drive the system into a true local minimum. Imaginary frequencies correspond to negative eigenvalues in the Hessian matrix and relate to unstable geometrical conformations. The self-consistency of the noninteractive wave function is performed with a convergence threshold on the density matrix of 10^{-6} and 10^{-8} for the root-mean-square and maximum-density-matrix error between iterations, respectively. These settings provide correct

* Corresponding authors. E-mail: (Balbuena) balbuena@tamu.edu; (Seminario) seminario@tamu.edu.
[†] Department of Chemical Engineering.
[‡] Department of Electrical and Computer Engineering.

10.1021/jp064691i CCC: $33.50
Published on Web 10/12/2006

TABLE 1: Structure and Energies for the Pt_n ($n = 1-5$) Cluster Using the B3PW91 Functional with the LANL2DZ and SDD Basis Sets[a]

		bond lengths (Å)		energy (Ha)		binding energy per atom (eV/atom)	
cluster	*m*	LANL	SDD	LANL	SDD	LANL	SDD
Pt_2	3	2.356 (2.33)[b]	2.528 (2.33)[b]	−238.33596	−238.76748	−1.35 (−1.57)[c]	−1.09 (−1.57)[c]
Pt_3	1	2.499 (2.66)[d]	2.499	−357.56049	−358.23354	−1.86	−1.83
Pt_4	5−3	$R_1 = 2.555$ $R_2 = 2.542$ $\theta = 120.4$	$R_1 = 2.551$ $R_2 = 2.702$ $\theta = 116.0$	−476.76396	−477.66073	−1.97	−1.94
Pt_5	5	1−2 = 2.493 1−3 = 3.143 1−4 = 2.612 1−5 = 2.549 2−3 = 2.513 3−4 = 2.540 4−5 = 2.489	1−2 = 2.504 1−3 = 2.636 1−4 = 2.636 1−5 = 2.504 2−3 = 2.568 3−4 = 2.652 4−5 = 2.568	−595.99458	−597.11328	−2.19	−2.14

[a] *m* is the multiplicity = $2S + 1$ where *S* is the total electron spin of the molecule; the ground state of Pt_4 was quintet using LANL2DZ and triplet with the SDD basis set; experimental values are indicated in parentheses. [b] Ref 42. [c] Ref 43. [d] Ref 44.

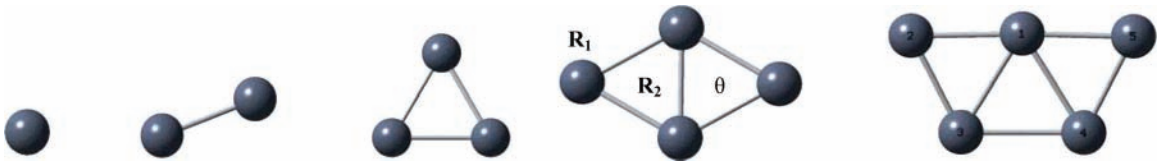

Figure 1. Smallest Pt clusters. Bond lengths and energies are shown in Table 1.

energies of at least five decimal figures, three for the atom lengths and one for the bond angles within the level of theory.

The calculations are performed using DFT as coded in the program Gaussian 03[16] by means of the B3PW91 hybrid functional, which uses a combination of the Becke3 (B3)[17] exchange functional and the Perdew−Wang (PW91)[18,19] correlation functional. The hybrid functional B3PW91 is used with the quasirelativistic pseudopotential and basis set LANL2DZ, which describes the 1*s* to 4*f* core electrons for Pt using effective core pseudopotentials of Hay−Wadt.[20−22] We also tried the Stuttgart−Dresden ECPs (SDD);[23] however, the results are not better for cases where experimental information is available. The SDD basis set practically uses primitive Gaussians for the valence electrons of heavy atoms and includes relativistic effects within Dirac−Fock theory.[24]

The continuum is considered through a combined Green function−density functional theory approach initially used to determine the electrical characteristics of single molecules trapped at metal or semiconductor junctions. This procedure went through a very intensive development[25−34] and has been adapted for the study of reactions on surfaces.[35−37] Bulk properties of platinum are calculated using Crystal-03.[38,39] Specifically, the total DOS is obtained through a Green function approach, whereby the bulk continuous DOS broadens and shifts the discrete MOs of the cluster, forming the total DOS of the cluster as affected by the bulk. The reader is forwarded to refs 29, 40 and references therein for further details regarding the theoretical methods used in this work.

III. Results and Discussion

We describe in this section the results on hydrogenated platinum clusters, followed by an analysis of the local DOS on platinum substrates and by a description of the oxygen contribution to the molecular orbitals.

Platinum Clusters. Clusters with different multiplicities are analyzed to determine the most stable structures, associatedwith the lowest energies. Geometries, multiplicities, energies, and binding energies per atom of the most stable structures of Pt_n ($n = 1-5$) clusters are shown in Table 1, and the corresponding structures are displayed in Figure 1. The LANL2DZ uses 22 basis functions per Pt atom; however, the SDD uses 39 basis functions for the 18 valence electrons of Pt. The binding energy per atom for a Pt_n cluster is calculated as done in ref 41:

$$E_B = (E(Pt_n) - n(E_{Pt}))/n$$

The comparison of results using LANL2DZ and SDD basis sets for the platinum dimer illustrates that the bond length obtained with LANL2DZ (2.356 Å) is closer to the experimental value (2.33 Å)[42] than that of SDD (2.528 Å). The ground state of the dimer is a triplet, and it is 1.64 eV more stable than the quintet state using LANL2DZ and 0.93 eV with the SDD basis set. Sebetci,[1] Yang, and Drabold[8] and Li and Balbuena[41] have reported the same ground state. Xiao and Wang[4] and Grönbeck and Andreoni[7] reported bond lengths of 2.34 and 2.32 Å, respectively, which are very similar to our results with the LANL2DZ basis set.

The experimental value[43] for the binding energy of Pt_2 is −1.57 eV/atom, which is overestimated by 0.22 eV/atom using LANL2DZ and by 0.48 eV using the SDD basis set. Reference 41 reported a value of −1.15 eV/atom, in very good agreement with our SDD results; however, different results were obtained in refs 1,4 of −1.68 and −1.76 eV/atom, respectively, in better agreement with the LANL2DZ results. Others have reported 2.37 Å[1] and 2.46 Å[2] for the bond length and −1.68 eV/atom for the binding energy.[1]

The optimized structure for Pt_3 is an equilateral triangle with symmetry D_{3h}, and both basis sets yield the same value for the bond length. In this case, there is not a marked difference between the singlet and triplet states. Nevertheless, the singlet is the ground state in agreement with previous work.[7,41] The bond lengths and binding energy agree with ref 41, but they are lower than the values reported by others.[4,8] Sebetci[1] has reported a distance of 2.53 Å and a binding energy of −2.19

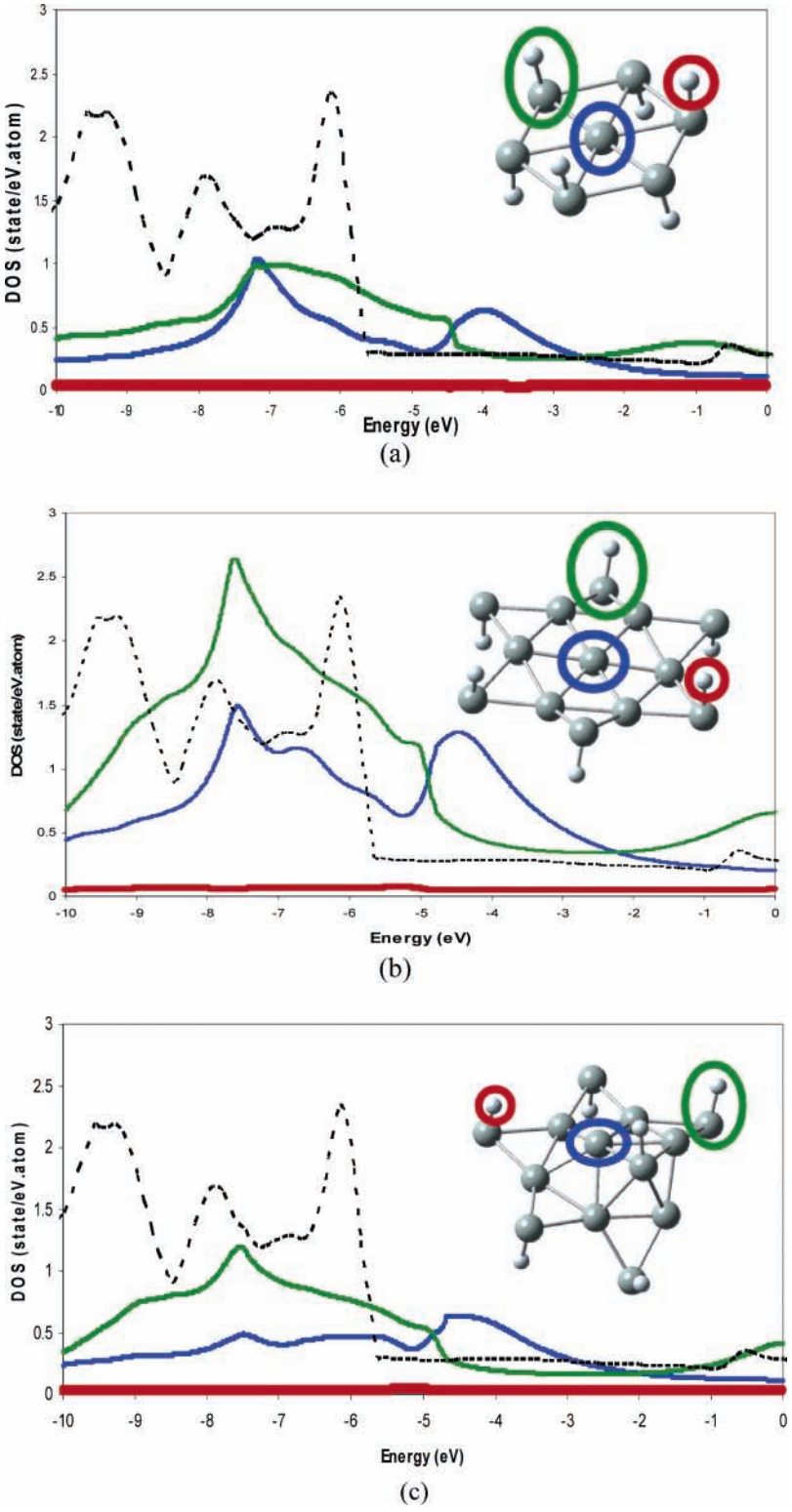

Figure 2. Local DOS plots corresponding to the top of the central Pt (blue), one of the Pt−H corners (green), and one of the hydrogen atoms (red) of (a) singlet Pt_7H_6, (b) triplet $Pt_{13}H_6$, and (c) singlet $Pt_{13}H_6$. Total DOS of Pt bulk (dotted line) obtained using Crystal-03 is also shown. All clusters are fully optimized and have no zero imaginary frequencies.

eV/atom by using the B3PW91/LANL2DZ level of theory. Our calculated bond-length values implementing the same method are 0.031 Å shorter, and all the calculated values are underestimated when compared with the experimental value of 2.66 Å.[44]

The bond lengths for the Pt_4 rhombus with symmetry D_{2h} are similar using both basis sets. The ground states are quintet and triplet using the LANL2DZ and SDD basis sets, respectively. References 1,8 reported an out-of-plane rhombus of C_{2v} point group with similar values of bond length but having comparatively greater binding energies. Our bond-length values are in agreement with ref 41, that reported the ground state for Pt_4 as singlet. BLYP calculations[7] have found an out-of-of-plane structure for triplet and a plane rhombus for singlet. Other references[7,45] reported the triplet as the ground state for the tetramer.

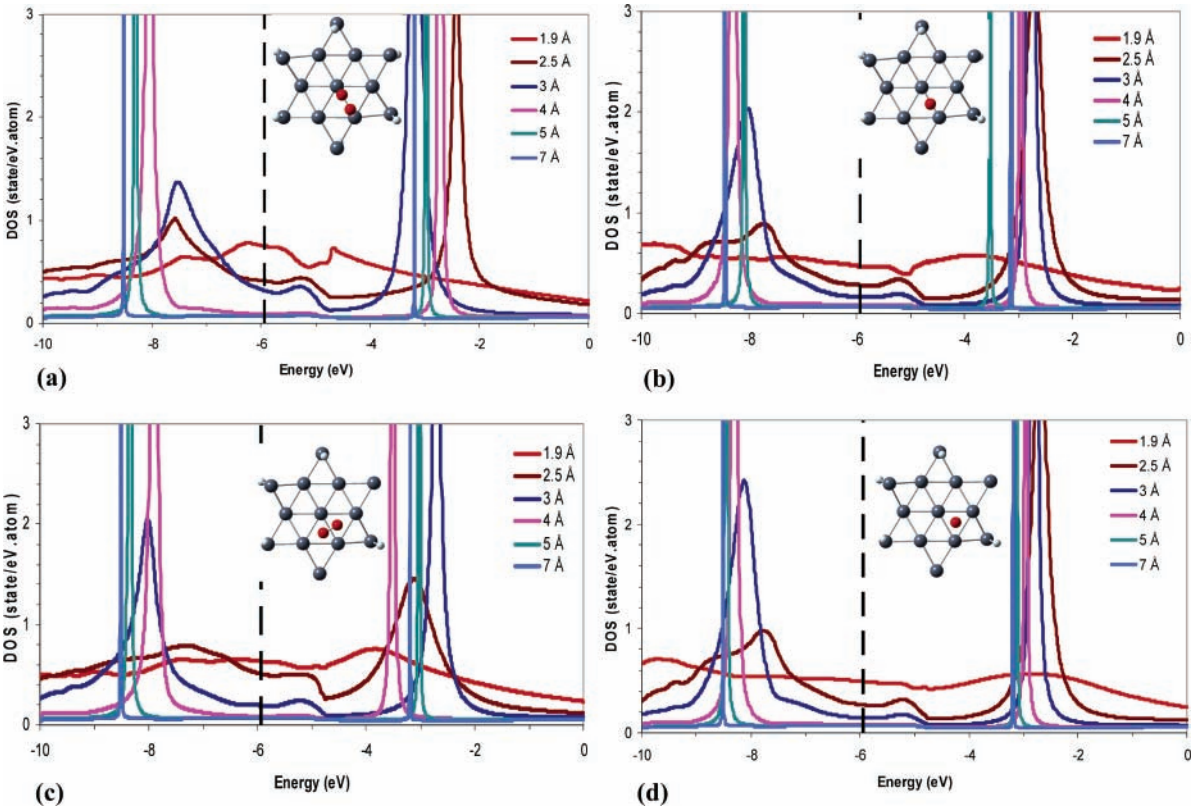

Figure 3. DOS of the complex $Pt_{13}H_6-O_2$ (all structures are triplets) for O_2 located at different distances from the surface: (a) O_2 parallel to the surface on a bridge site, (b) O_2 perpendicular to the surface on a bridge site, (c) O_2 parallel to the surface on a bridge, and (d) O_2 perpendicular to the surface on a hollow site. The Fermi level of Pt[46] is indicated by the dashed black line. The O−O bond length is kept at its vacuum value (1.2 Å), and the electronic structures are obtained at these single-point geometries.

The lowest energy of Pt_5 corresponds unambiguously to the quintet state. Sebetci[1] has found the quintet state for a bridge-site-capped tetrahedron and a rhombus pyramid but the triplet state for a W-like geometry as the structure reported in this work. The septet is the second structure more stable, and it is 0.22 eV higher than the quintet state using the LANL2DZ and 0.30 eV using the SDD. The bond lengths are similar to values calculated by other authors.[1,7,8,41] The binding energy calculated by using the SDD basis set is in agreement with that of ref 41, but refs 1,4,8 reported larger binding energies.

The convenience of using the LANL2DZ instead of the SDD basis sets and effective core potentials is inferred from the above discussion. Thus, we adopted the B3PW91/LANL2DZ level of theory for the calculations reported in the following sections in this manuscript.

Local DOS on a Platinum Surface. Figure 2 shows the local DOS corresponding to specific sites of hydrogen-passivated surfaces belonging to stable cluster structures. Adding hydrogen atoms, it is possible to obtain true local minima, which are very difficult to find for small structures resembling a Pt(111) surface. Three sites are analyzed in each of the clusters. For Pt_7H_6, these local sites correspond to a central Pt atom (within the blue circle in Figure 2a), hydrogen at the periphery of the cluster (red circle), and the Pt−H bond region (green circle). The DOS on the central Pt site of the triplet $Pt_{13}H_6$ (Figure 2b) shows the closest resemblance to the Pt bulk total DOS, indicated by the dotted curve. The differences between the DOS at the central site and the total bulk DOS, except for a scaling factor, are due to the fact that the metal atoms belong to a single-layer surface and not to the bulk, and also to the small size of the cluster. Figure 2c shows the results for the singlet $Pt_{13}H_6$ showing that as the surface distorts from a (111) the DOS tends to be constant. At the Pt−H site the bulk features are distorted, and they practically disappear at the hydrogen sites for the three clusters in Figure 2. To improve the effect of the finite size of the surface, we tested larger clusters, which are useful for investigating reactions at realistic sites. Notice that the two $Pt_{13}H_6$ clusters (single and triplet) allow analyzing chemical reactions within the central seven atoms with little or no interference from the edges or from the hydrogen atoms.

Local DOS of Reacting Oxygen on Different Surface Sites. Figure 3 shows the local DOS at different sites on $Pt_{13}H_6$ interacting with a ground-state O_2 molecule (triplet) located at several distances from the surface. The various distances represent a molecule approaching the surface; however, the O_2 geometry is kept fixed (the O−O distance is 1.2 Å in all cases). At the closest distances the effect of the surface is clearly dominant, the 1.9-Å distance represents an unphysical situation since at such short distances the O_2 molecule should start dissociating and possibly chemisorbing, but at 2.5 and 3 Å the *d*-band peak is observed at the left of the Fermi level denoting a certain degree of interaction molecule/surface.

As O_2 separates farther from the surface, its local DOS reveals the discrete molecular orbital energies represented by the peaked curves (4, 5, and 7 Å) in Figure 3. The minimum energy for the bridge configuration (Figure 3a) corresponds to a 7-Å separation of O_2 from the surface; however, this energy surface is a shallow minimum as the energy difference is 0.018 and 0.075 eV lower than those at 4 and 5 Å, respectively. On the other hand, the lowest energy is found at 4 Å for O_2 perpendicular to the surface (Figure 3b,d), the difference with the parallel case is because in the perpendicular position the second oxygen atom is 1.2 Å farther from the surface, and thus the isolated oxygen molecule geometry may still be possible.

The lowest energy for the O_2 located in the geometry depicted in Figure 3c is found at 5 Å. Note that when O_2 lies

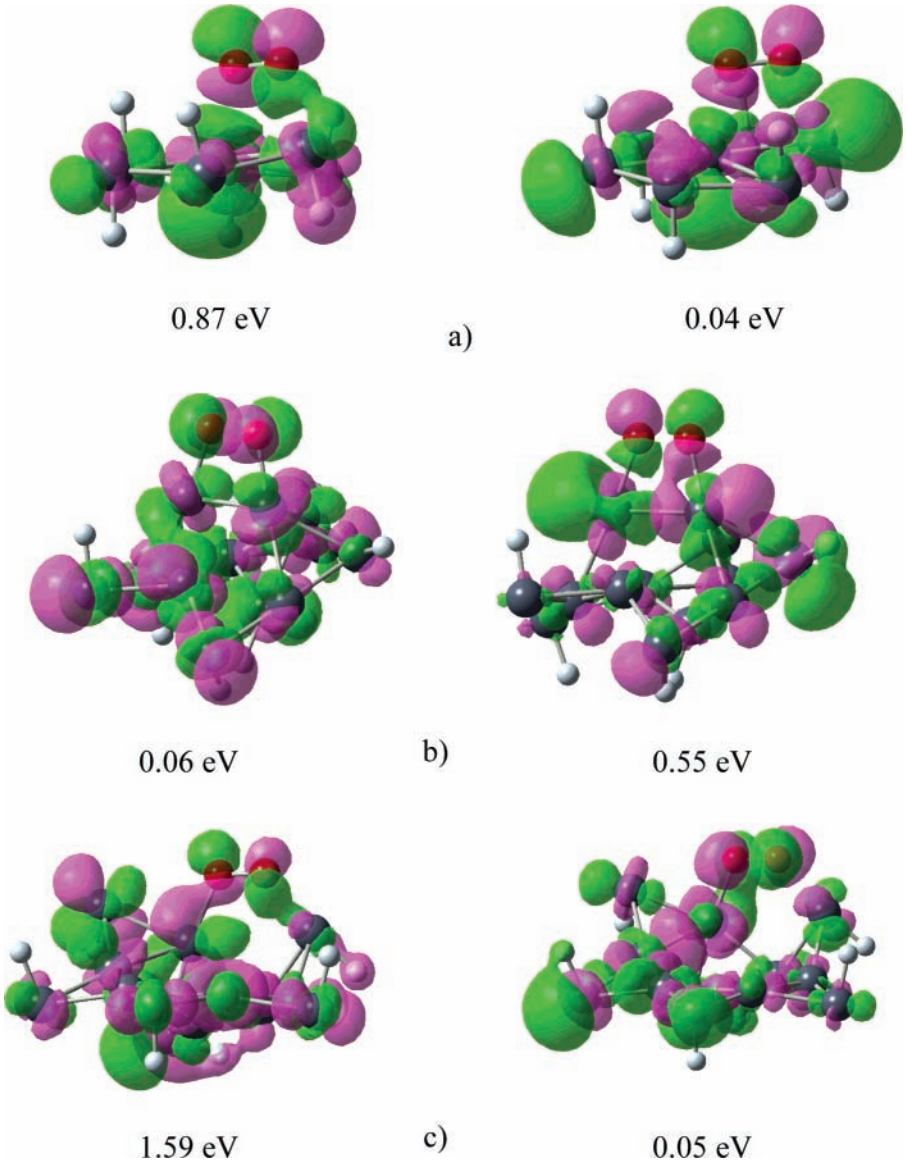

Figure 4. Nearest occupied and unoccupied molecular orbitals to the HOMO (left) and LUMO (right), respectively, including their relative energy separations or barriers calculated with respect to the HOMO and LUMO, respectively. The molecular orbitals correspond to isovalues of 0.02 au (a) triplet $Pt_7H_6-O_2$, (b) singlet $Pt_{13}H_6-O_2$, and (c) triplet $Pt_{13}H_6-O_2$. All complexes are fully optimized without any geometrical constraint using the B3PW91/LANL2DZ level of theory, showing no imaginary frequencies.

perpendicular to the surface (Figure 3b,d) and in the case of Figure 3c, the *d*-band peaks (at 3 Å, blue curves) are shifted to lower energies compared to those of Figure 3a, becoming more distant from the Fermi level and suggesting a diminished reactivity associated with those complexes because of their unfavorable geometry. Thus, varying the O_2 position with respect to the surface clearly shows the connection between geometry and electronic structure of the adsorbate−cluster system.

Finally, we calculate the fully optimized structures of the complexes $Pt_7H_6-O_2$ and $Pt_{13}H_6-O_2$ and run second-derivative calculations to make sure that they correspond to local minima. The lowest energies corresponded to a triplet for $Pt_7H_6-O_2$. An unstable singlet is found at 12.4 kcal/mol above the triplet and with an imaginary frequency of $65i$ cm^{-1}. However for $Pt_{13}H_6-O_2$, few conformations yield local minima. The most relevant are the following. (a) These are the singlet and triplet obtained by adding O_2 to the triplet conformation of $Pt_{13}H_6$, which had a planar structure. This yields another singlet as the lowest structure; however, the corresponding triplet is only 3.1 kcal/mol above the singlet. The triplet shows one imaginary frequency of only $13i$ cm^{-1}, which perhaps can be disregarded as unstable. (b)These are the singlet and triplet obtained when adding O_2 to the triplet deformed geometry of $Pt_{13}H_6$ (Figure 2). Both, a singlet and a triplet complexes yield local minima with the triplet lower than the singlet by 3.3 kcal/mol.

Interestingly, the highest occupied molecular orbitals of these three structures have very similar energy eigenvalues, −5.85, −5.86, and −5.74 eV, and all these values are very similar to the Fermi level of bulk platinum (∼−6.0 eV) yielding a continuity in energy between clusters and bulk that perhaps allows us to model the bulk. This is justified by the fact that very small clusters have been used already to model reactions on bulk and yielded acceptable agreement with experiments. On the other hand, the lowest unoccupied molecular orbitals of these complexes also yield very similar energies, −4.21, −4.62, and −4.38 eV, yielding an average gap of roughly 1.4 eV, which means that these nanoclusters actually become semiconductors.

The specific effect of O_2 on the molecular orbitals of the clusters can be observed in Figure 4, which shows the occupied and unoccupied molecular orbitals nearest to the HOMO and LUMO, respectively, including their relative energy separations

or barriers. The HOMO and LUMO of O_2 in its ground state are π-type antibonding MOs; interestingly, these similar MOs are well-separated in energy due to their occupation (∼13 eV). A significant interaction of the antibonding π^* MOs of oxygen with combination of *d*-type molecular orbitals of the cluster is clearly shown for all complexes. Also notice that in all cases, at least one of the MOs is practically at the same energy level as the HOMO or LUMO of the complex. This coupling of the MOs from the molecule and the cluster definitely has an effect on chemical reactivity, in this case inducing dissociation of the O−O bond by allowing practically barrierless electron transfer between cluster and molecule.

Moreover, beyond chemical reactivity, the coupling of the MOs of the molecule and the cluster is responsible for transferring vibrational spectral signatures from the small molecule to the larger cluster. Thus, exciting the cluster−molecule complex yields a relatively much larger cross section for detection than if a detection beam were directed only to the individual molecule; this is always the case if the radiation source has much larger wavelengths than the size of the molecule, and then a strong enhancement of the detection signal takes place. This concept is of paramount importance for the detection of a small number of molecules.

IV. Conclusions

We developed a few relatively small platinum testbeds to study catalytic reactions. These surfaces may include the contribution from a bulk continuum or may simply represent a local site on a nanocluster or bulk. Given the correspondence between molecular orbital energies and bulk properties, these nanoclusters are good models to represent the local chemistry. In this particular case, the requirement is that a stable cluster may be connected to a stable bulk with equivalent Fermi level and highest occupied molecular orbital, respectively. The interaction of platinum clusters with molecular oxygen yields a complex cluster−molecule with fully delocalized molecular orbitals with energies in the neighborhood of the Fermi energy of platinum. This is responsible for the interesting catalytic behavior of this material. Always one of the fully delocalized complex molecular orbitals is practically at the same energy of the HOMO or LUMO energies of the complex. We demonstrate a clear connection between the geometry of the molecule−cluster interface and electronic structure. Pt has the lowest Fermi level (∼−6 V) of any structure made of single elements from the periodic table; we showed that even these small clusters show a HOMO energy in the same neighborhood. Thus, we may conclude that any molecule whose MOs are able to strongly entangle with those of a Pt cluster yielding MOs at energy values of ∼−6 eV are strong candidates to experience bond dissociation upon interaction with the platinum cluster. An important additional application of this concept is the design of metal clusters with relatively much larger cross-sections than small single molecules, allowing the detection of small molecules by detection of the complex via vibrational spectroscopy.

Acknowledgment. We acknowledge financial support from the Department of Energy/Basic Energy Sciences, (DE-FG02-05ER15729) as well as from the U.S. Army Research Office and the U.S. Defense Threat Reduction Agency (DTRA). J.M.S. thanks the kindness of the Fox family for the endowed Lannater and Herb Fox Professorship.

References and Notes

(1) Greeley, J.; Norskov, J. K.; Mavrikakis, M. Electronic structure and catalysis on metal surfaces. *Ann. Rev. Phys. Chem.* **2002**, *53*, 319−348.

(2) Balasubramanian, K. Electronic states of Pt_2. *J. Chem. Phys.* **1987**, *87*, 6573−6578.

(3) Balasubramanian, K. CASSCF/CI calculations of electronic states and potential energy surfaces of PtH_2. *J. Chem. Phys.* **1987**, *87*, 2800−2805.

(4) Xiao, L.; Wang, L. Structures of platinum clusters: Planar or spherical? *J. Phys. Chem. A* **2004**, *108*, 8605−8614.

(5) Andrews, L.; Wang, X.; Manceron, L. Infrared spectra and density functional calculations of platinum hydrides. *J. Chem. Phys.* **2001**, *114*, 1559−1566.

(6) Sebetci, A.; Guvenc, Z. B. Energetics and structures of small clusters: Pt_n, $n = 2-21$. *Surf. Sci.* **2003**, *525*, 66−84.

(7) Gronbeck, H.; Andreoni, W. Gold and platinum microclusters and their anions: Comparison of structural and electronic properties. *Chem. Phys.* **2000**, *262*, 1−14.

(8) Yang, S. H.; Drabold, D. A.; Adams, J. B.; Ordejon, P.; Glassford, K. Density funtional studies of small platinum clusters. *J. Phys.: Condens. Matter* **1997**, *9*, L39−L45.

(9) Balasubramanian, K.; Feng, P. Y. Potential-energy surfaces for Pt_2+H and Pt+H interactions. *J. Chem. Phys.* **1990**, *92*, 541−550.

(10) Wang, H.; Carter, E. Metal−metal bonding in transition-metal clusters with open d shells: Pt_3. *J. Phys. Chem.* **1992**, *96*, 1197−1204.

(11) Tian, W. Q.; Ge, M.; Sahu, B. R.; Wang, D.; Yamada, T.; Mashiko, S. Geometrical and electronic structure of the Pt7 cluster: A density functional study. *J. Phys. Chem.* **2004**, *108*, 3806−3812.

(12) Wang, S. W.; Pitzer, K. S. The ground and excited states of PtH and PtH^+ by relativistic ab initio electronic structure calculations: A model study for hydrogen chemisorption on platinum surfaces and related photoemission properties. *J. Chem. Phys.* **1983**, *79*, 3851−3858.

(13) Okamoto, Y. Density functional calculations of atomic and molecular adsorptions on 55-atom metal clusters: Comparison with (111) surfaces. *Chem. Phys. Lett.* **2005**, *405*, 79−83.

(14) Koper, M. T. M.; Shubina, T. E.; Santen, R. A. v. Periodic density funtional study of CO and OH adsorption on Pt−Ru alloy surfaces: Implications for CO tolerant fuel cell catalysts. *J. Phys. Chem. B* **2002**, *106*, 686−692.

(15) Schlegel, H. B. Optimization of equilibrium geometries and transition structures. *J. Comput. Chem.* **1982**, *3*, 214−218.

(16) Frisch, M. J.; Trucks, G. W.; Schlegel, H. B.; Scuseria, G. E.; Robb, M. A.; Cheeseman, J. R.; Montgomery, J. A.; Vreven, T., Jr.; Kudin, K. N.; Burant, J. C.; Millam, J. M.; Iyengar, S. S.; Tomasi, J.; Barone, V.; Mennucci, B.; Cossi, M.; Scalmani, G.; Rega, N.; Petersson, G. A.; Nakatsuji, H.; Hada, M.; Ehara, M.; Toyota, K.; Fukuda, R.; Hasegawa, J.; Ishida, M.; Nakajima, T.; Honda, Y.; Kitao, O.; Nakai, H.; Klene, M.; Li, X.; Knox, J. E.; Hratchian, H. P.; Cross, J. B.; Adamo, C.; Jaramillo, J.; Gomperts, R.; Stratmann, R. E.; Yazyev, O.; Austin, A. J.; Cammi, R.; Pomelli, C.; Ochterski, J. W.; Ayala, P. Y.; Morokuma, K.; Voth, G. A.; Salvador, P.; Dannenberg, J. J.; Zakrzewski, V. G.; Dapprich, S.; Daniels, A. D.; Strain, M. C.; Farkas, O.; Malick, D. K.; Rabuck, A. D.; Raghavachari, K.; Foresman, J. B.; Ortiz, J. V.; Cui, Q.; Baboul, A. G.; Clifford, S.; Cioslowski, J.; Stefanov, B. B.; Liu, G.; Liashenko, A.; Piskorz, P.; Komaromi, I.; Martin, R. L.; Fox, D. J.; Keith, T.; Al-Laham, M. A.; Peng, C. Y.; Nanayakkara, A.; Challacombe, M.; Gill, P. M. W.; Johnson, B.; Chen, W.; Wong, M. W.; Gonzalez, C.; Pople, J. A. *Gaussian-2003*, revision B.4; Gaussian, Inc.: Pittsburgh, PA, 2003.

(17) Becke, A. D. A new mixing of Hartree−Fock and local density-functional theories. *J. Chem. Phys.* **1993**, *98*, 1372−1377.

(18) Perdew, J. P.; Chevary, J. A.; Vosko, S. H.; Jackson, K. A.; Pederson, M. R.; Singh, D. J.; Fiolhais, C. Atoms, molecules, solids, and surfaces: Applications of the generalized gradient approximation for exchange and correlation. *Phys. Rev. B* **1992**, *46*, 6671−6687.

(19) Perdew, J. P.; Wang, Y. Accurate and simple analytic representation of the electron-gas correlation energy. *Phys. Rev. B* **1992**, *45*, 13244−13249.

(20) Wadt, W. R.; Hay, P. J. Ab initio effective core potentials for molecular calculations. Potentals for main group elements Na to Bi. *J. Chem. Phys.* **1985**, *82*, 284−298.

(21) Hay, P. J.; Wadt, W. R. Ab initio effective core potentials for molecular calculations. Potentials for the transition metal atoms Sc to Hg. *J. Chem. Phys.* **1985**, *82*, 270−283.

(22) Hay, P. J. Gaussian basis sets for molecular calculations. The representation of 3d orbitals in transition-metal atoms. *J. Chem. Phys.* **1977**, *66*, 4377−4384.

(23) Andrae, D.; Haussermann, U.; Dolg, M.; Stoll, H.; Preuss, H. Energy-adjusted ab initio pseudopotentials for the 2nd-row and 3rd-row transition elements: Molecular test for Ag_2, Au_2 and RuH, OsH. *Theor. Chim. Acta* **1990**, *78*, 247−266.

(24) Fuentealba, P.; Stoll, H.; von Szentpaly, L.; Schwerdtfeger, P.; Preuss, H. On the reliability of semiempirical pseudopotentials: Simulation of Hartree−Fock and Dirac−Fock results. *J. Phys. B* **1983**, *16*, L323−L328.

(25) Seminario, J. M.; Zacarias, A. G.; Tour, J. M. Molecular current−voltage characteristics. *J. Phys. Chem. A* **1999**, *103*, 7883−7887.

(26) Derosa, P. A.; Seminario, J. M. Electron transport through single molecules: Scattering treatment using density functional and green function theories. *J. Phys. Chem. B* **2001**, *105*, 471−481.

(27) Seminario, J. M.; De La Cruz, C. E.; Derosa, P. A. A theoretical analysis of metal-molecule contacts. *J. Am. Chem. Soc.* **2001**, *123*, 5616−5617.

(28) Seminario, J. M.; Zacarias, A. G.; Derosa, P. A. Analysis of a dinitro-based molecular device. *J. Chem. Phys.* **2002**, *116*, 1671−1683.

(29) Seminario, J. M.; Cordova, L. E.; Derosa, P. A. An ab initio approach to the calculation of current−voltage characteristics of programmable molecular devices. *Proc. IEEE* **2003**, *91*, 1958−1975.

(30) Seminario, J. M. Practical aspects of electron transport through single molecules. *Proc. IEEE Nanotech. Conf.* **2004**, 4.

(31) Seminario, J. M.; De La Cruz, C.; Derosa, P. A.; Yan, L. Nanometer-size conducting and insulating molecular devices. *J. Phys. Chem. B* **2004**, *108*, 17879−17885.

(32) Seminario, J. M. Molecular electronics: Approaching reality. *Nat. Mater.* **2005**, *4*, 111−113.

(33) Seminario, J. M.; Yan, L. Ab initio analysis of electron currents in thioalkanes. *Int. J. Quantum Chem.* **2005**, *102*, 711−723.

(34) Seminario, J. M.; Yan, L.; Ma, Y. Scenarios for molecular-level signal processing. *Proc. IEEE* **2005**, *93*, 1753−1764.

(35) Balbuena, P. B.; A. D., Agapito, L. A.; Seminario, J. M. Theoretical analysis of oxygen adsorption on Pt-based clusters alloyed with Co, Ni, or Cr embedded in a Pt matrix. *J. Phys. Chem. B* **2003**, *107*, 13671−13680.

(36) Balbuena, P. B.; Altomare, D.; Vadlamani, N.; Bingi, S.; Agapito, L. A.; Seminario, J. M. Adsorption of O, OH, and H_2O on Pt-based bimetallic clusters alloyed with Co, Cr, and Ni. *J. Phys. Chem. A* **2004**, *108*, 6378−6384.

(37) Seminario, J. M.; Ma, Y.; Agapito, L. A.; Yan, L.; Araujo, R. A.; Bingi, S.; Vadlamani, N. S.; Chagarlamudi, K.; Sudarshan, T. S.; Myrick, M. L.; Colavita, P. E.; Franzon, P. D.; Nackashi, D. P.; Cheng, L.; Yao, Y.; Tour, J. M. Clustering effects on discontinuous gold film nano cells. *J. Nanosci. Nanotech.* **2004**, *4*, 907−917.

(38) Roetti, C. The Crystal Code. In *Quantum-Mechanical ab initio Calculation of the Properties of Crystalline Materials*; Pisani, C., Ed.; Springer-Verlag: Berlin, 1996; p 67.

(39) Dovesi, R.; Causa, M.; Orlando, R.; Roetti, C.; Saunders, V. R. Ab initio approach to molecular-crystals − A periodic Hartree−Fock study of crystalline urea. *J. Chem. Phys.* **1990**, *92*, 7402−7411.

(40) Seminario, J. M. A theory guided approach to molecular electronics. *Proc. IEEE Nanotech. Conf.* **2003**, *3*, 75−78.

(41) Li, T.; Balbuena, P. B. Computational studies of the interactions of oxygen with platinum clusters. *J. Phys. Chem. B* **2001**, *105*, 9943−9952.

(42) Airola, M. B.; Morse, M. D. Rotationally resolved spectroscopy of Pt_2. *J. Chem. Phys.* **2002**, *116*, 1313−1317.

(43) Taylor, S.; Lemire, G. W.; Hamrick, Y. M.; Fu, Z.; Morse, M. D. Resonant two-photon ionization spectroscopy of jet-cooled Pt_2. *J. Chem. Phys.* **1988**, *89*, 5517−5523.

(44) Muller, U.; Sattler, K.; Xhie, J.; Venkateswaran, N.; Raina, G. Scanning tunneling microscopy of single platinum atoms and small platinum clusters on highly oriented pyrolytic graphite. *J. Vac. Sci. Technol. B* **1991**, *9*, 829−832.

(45) Dai, D.; Balasubramanian, K. Electronic structures of Pd_4 and Pt_4. *J. Chem. Phys.* **1995**, *103*, 648−655.

(46) *CRC Handbook of Chemistry and Physics*; Lide, D. R., Ed.; CRC Press: Boca Raton, FL, 2005.